Supplementary Material

S. 1   Algorithm and parameter values for agent-based model

(a) *Initialization.* We consider an idealised initial condition unless otherwise specified: lattice points (x, y), for which $x < D/4$ or $x > 3D/4$, are occupied by an agent.

(b) *Update algorithm.* Let $N(t)$ denote the number of agents at time t. To update the agent-based model at time t to the next simulation time $t + \tau$, we do the following:

1. First, $N(t)$ agents are chosen sequentially at random and given the opportunity to move. An agent at (x, y) attempts to move with probability p_m to $(x \pm \Delta, y)$ or $(x, y \pm \Delta)$, with the target site chosen with equal probability.

2. $N(t)$ agents are then selected sequentially at random again and given the opportunity to proliferate. An agent at (x, y) attempts to proliferate with probability p_p and places its daughter agent at $(x \pm \Delta, y)$ or $(x, y \pm \Delta)$, target sites being chosen with equal probability.

At each update time, agents can move and/or proliferate only if the target site is vacant. A list of the parameters that are used in the agent-based model is presented in Table S1.

Parameter	Description	Value	Units
p_m	Motility probability	0.3	N/A
p_p	Proliferation probability	0.1	N/A
T	End time	24	hr
τ	Time step	0.01	hr
D	Domain length	500	μm
Δ	Lattice spacing	10	μm

Table S1: List of the parameters used in the agent-based model, together with their default values.

S. 2 Objective function for optimal window size

We describe the objective function to calculate the optimal window size in detail. Let us consider a window size w and divide Y, which has size D, into $M = D/w$ segments of length w, denoted by Y_s for $1 \leq s \leq M$. Y_s is the set of pixels that belong to a segment of length w. When D is not divisible by w, Y is divided into $M = \lfloor \frac{Y}{w} \rfloor + 1$ segments, where the first $\lfloor \frac{Y}{w} \rfloor$ segments have length w and the last one has length $D - w \times \lfloor \frac{D}{w} \rfloor$. After applying the linear approximation with respect to the window size w, we have the following approximation for the interface position at time t_n for each $j \in Y_s$,

$$i_j(t_n) \approx m_s t_n + b_s, \tag{S1}$$

where m_s and b_s are determined as described in Section 2.4. We consider the following fitness functions that evaluate the interface position approximation (S1):

1. Residual sum of squares

$$E(w) = \frac{1}{2D} \sum_{j=1}^{D} \sum_{n=1}^{N^*} \left(e_{l,j,n}{}^2 + e_{r,j,n}{}^2 \right) \tag{S2}$$

   where $e_{l,j,n} = i_j(t_n) - (m_s t_n + b_s)$ is the residual at time t_n for $j \in Y_s$ of the linear approximation (S1). The first subscript denotes the interface (left or right). N^* denotes the time point when the two interfaces meet.

2. Linear fitness

$$R(w) = \frac{1}{2D} \sum_{j=1}^{D} R_{lj}^2 + R_{rj}^2 \tag{S3}$$

   where R_{lj}^2 is the coefficient of determination R^2 of the linear approximation to the j-th coordinate of the left interface position progress over time, i.e. let $\overline{i_j}(t_n) = \frac{1}{N^*} \sum_{n=1}^{N^*} i_j(t_n)$, $SS_{tol} = \sum_{n=1}^{N^*} (i_j(t_n) - \overline{i_j})^2$ and $SS_{res} = \sum_{n=1}^{N^*} (m_s t_n + b_s - i_j(t_n))^2$, then $R_{lj}^2 := 1 - \frac{SS_{res}}{SS_{tol}}$. The better the overall linear fit, the closer Fit_{R^2} should be to 1. The subscript denotes the interface (left or right).

3. Fitness between left and right velocities
   We consider a distance metric derived from the Kolmogorov-Smirnov test statistic [1]. Given two data sets $\{a_s\}_{s=1}^{n}$ and $\{b_r\}_{r=1}^{m}$ and their empirical cumulative distributions F_n and F_m, respectively, the Kolmogorov-Smirnov statistic is:

$$D_{n,m} = \sup_{x \in \mathbb{R}} |F_n(x) - F_m(x)|. \tag{S4}$$

   Normalizing the statistic by the effective number of data points, we obtain the KS distance that was introduced in [4]:

$$Dist(\{a_s\}_{s=1}^{n}, \{b_r\}_{r=1}^{m}) = \frac{nm}{n+m} D_{n,m}, \tag{S5}$$

   where $\{a_s\}_{s=1}^{n}$, $\{b_r\}_{r=1}^{m}$ are two ordered data points. We consider the $KS_{distance}$ between the left and right windowed velocity distributions

$$KS_{distance}(w) = Dist\left(\{m_l\}, \{m_r\}\right), \tag{S6}$$

   where the subscripts denote the left and right side, respectively. Ideally, the left and right windowed velocity distribution should be the smallest possible.

We consider the following global function:

$$\hat{F}(w) = Fit_{resid}(w) + Fit_{Rsquared}(w) + Fit_{KS_{distance}}(w), \qquad (S7)$$

where

$$Fit_{resid}(w) := \frac{\max\limits_{1 \le w \le D} E(w) - E(w)}{\max\limits_{1 \le w \le D} E(w) - \min\limits_{1 \le w \le D} E(w)}, \qquad (S8)$$

$$Fit_{Rsquared}(w) := \frac{R(w) - \min\limits_{1 \le w \le D} R(w)}{\max\limits_{1 \le w \le D} R(w) - \min\limits_{1 \le w \le D} R(w)}, \qquad (S9)$$

and

$$Fit_{KS_{distance}}(w) := \frac{\max\limits_{1 \le w \le D} KS_{distance}(w) - KS_{distance}(w)}{\max\limits_{1 \le w \le D} KS_{distance}(w) - \min\limits_{1 \le w \le D} KS_{distance}(w)}. \qquad (S10)$$

The terms are normalized so each term is between 0 and 1 and the largest value is the one maximizing each criterion. The global fitness function is normalized, $F(w) = \frac{1}{3}\hat{F}(w)$, such that $0 \le F(w) \le 1$. The width of the window with the largest $F(w)$ value is considered the optimal value with respect to the three fitness functions, weighted equally through the global function.

If additional scratches are considered to calculate the optimal window, we take a weighted sum of objective functions for each of the scratches considered. In such cases, the objective function can be written as

$$F(w) = \frac{1}{S} \sum_{s=1}^{n} F_s(w), \qquad (S11)$$

where F_s is the individual objective function for scratch assay s and S is the number of scratch assays considered.

S. 2.1 Similarity between left and right velocities

In this subsection we discuss why similarity between the left and right velocities is necessary for optimal window size calculation.

If the term $Fit_{KS_{distance}}$ is neglected when calculating the objective function (Equation (S7)), then the optimal window size will be a window of size $1\mu m$ since the front position is not averaged over a window and the actual interface position is considered for the linear fit, reducing the overall fitness error. We can observe this behaviour for the in vitro data in Figure S6 (a) and (b) where the fitness increases as the window size decreases. We now outline the problems of considering a window of size significantly smaller than the cell diameter.

For windows of size significantly smaller than the cell diameter, velocity values are correlated (See Figure S1 (a) and (b)) and not amenable to standard statistical analysis. In order to apply standard statistical tests, the velocities must have the same statistics as an independent and identically distributed (iid) sequence. One way to test for iid sequences is to consider the sample autocorrelation function [2] which, for an iid sequence with n elements and finite variance, gives approximately iid values that follow a normal distribution $\mathcal{N}(0, 1/n)$ [3]. A general observation from the in silico and in vitro data is that the autocorrelation function values from velocities corresponding to windows of size significantly smaller than the cell diameter differ greatly from an iid sequence. On the other hand, when considering windows whose sizes are similar to that of the cell diameter, the autocorrelation function resembles one for an iid sequence. To illustrate this, we simulate our agent-based model with the parameters in Table S1. We plot the autocorrelation function of the left velocities for windows of sizes $1, 2, 10$ and $12\mu m$ in Figure S1. The horizontal red lines in each plot delimit the 95% confidence interval from a normal distribution $\mathcal{N}(0, 1/n)$ where n is the number of velocities. We observe that for windows of size smaller than the cell diameter (1 and $2\mu m$), the autocorrelation values exceed the upper limit of the confidence interval and decrease slightly as the lag increases (see Figure S1 (a) and (b)). On the other hand, for velocities with windows of sizes similar to that of the cell diameter, most of the autocorrelation values are within the 95% confidence interval and as such can be considered to belong to an iid sequence (See Figure S1 (c) and (d)).

Another problem with windows of size significantly smaller than the cell diameter is that the velocity values of individual cells at the leading edge are over-represented and affect the overall distribution. This effect can be analysed by looking at the similarity between the left and right velocities of the in vitro and in silico data. Since the cells on each side come from a common monolayer, they are subject to the same biological conditions. As such, we expect the velocities from the left and right sides to exhibit the same statistics. A general observation from the in silico and in vitro data is that for windows of size significantly smaller than the cell diameter, the velocity distributions of each side differ while for windows whose sizes are similar to that of the cell diameter, the distributions more closely resemble each other. To illustrate this, we simulate the agent-based model with the parameters in Table S1. Violin plots of the velocity distributions for the left and right velocities corresponding to windows of size $1, 2, 10$ and $12\mu m$ are presented in Figure S2 (b). For windows that are smaller than the cell diameter, the velocity distribution of the left and right interfaces differ but for windows whose size are similar to that of the cell diameter, the distributions are more similar. The similarity between the left and the right velocity distributions can be quantified using the Kolmogorov Smirnov (KS) distance, Equation (S6). In Figure S2 (a) we plot the mean KS distance between the left and right velocities for 150 simulations of the agent based model using the parameter values listed in Table S1, we observe that the mean KS distance decreases as the window size increases.

We account for the statistical problems associated with windows which are significantly smaller than the cell diameter, by including the KS distance in the objective function. We evaluated this objective function for an agent-based model in which the cells only move horizontally in the direction of the scratch. In this case, the optimal window size is the cell diameter and this window gave the best fit and the best similarity between the left and right velocities (results not shown). Deviations

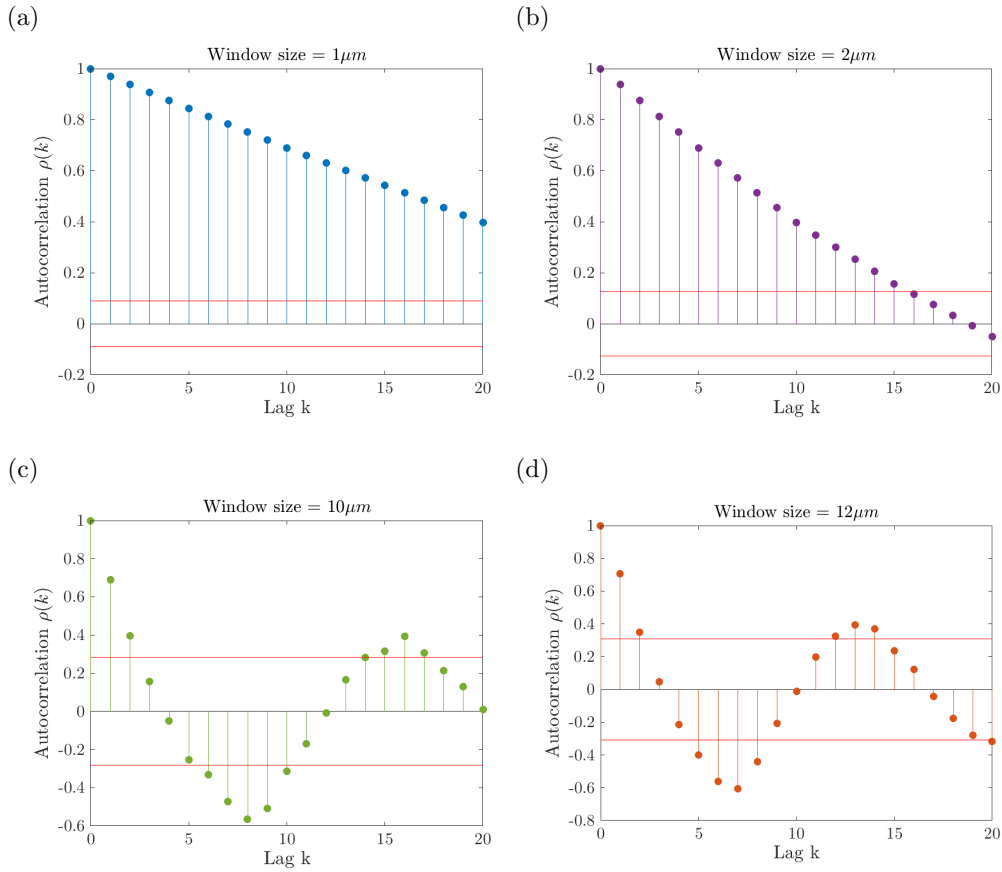from this result indicates lateral movement of the cells.

Figure S1: Plot of sample autocorrelation functions of left velocities corresponding to different window sizes for an agent-based simulation with the parameters in Table S1. We consider windows of size: (a) 1, (b) 2, (c) 10 and (d) $12\mu m$. The velocities show high correlation between neighbors for windows of size significantly smaller than the cell diameter, while for windows whose sizes are similar to that of the cell diameter, the autocorrelation values are within the expected confidence interval of an iid sequence that follow a normal distribution $\mathcal{N}(0, 1/n)$ where n is the number of velocities.
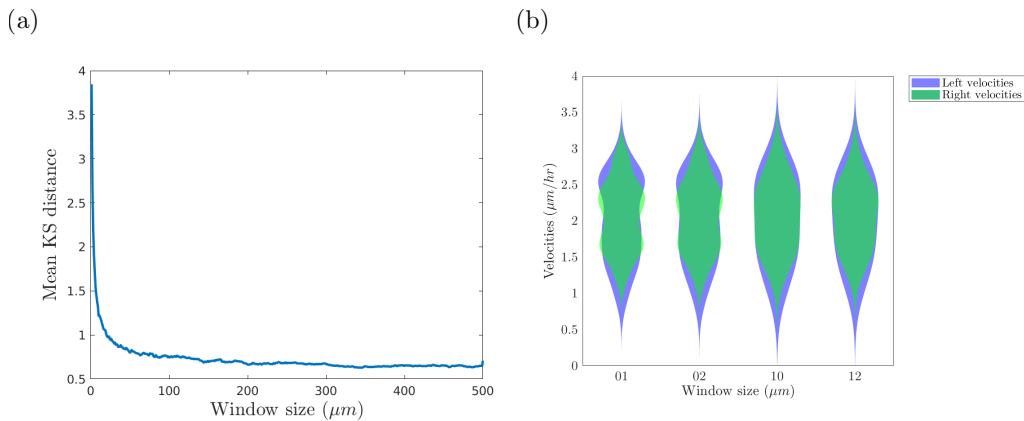

Figure S2: (a) Mean KS distance for the left and right velocity distributions while varying the window size. (b) Violin plots of the left and right velocities in blue and green, respectively, for different windows of size: 1, 2, 10 and 12 μm.

5

S. 3   Classification tests using in silico data

We present the results of the classification tests for the three quantification methods with respect to the focal parameter $\hat{P}$ with values in $\{0.1, 0.5, 0.9\} \times \{0.01, 0.09\}$. We consider $n = 4$ simulations as the sample size for our test and repeat the classification test 20 times.
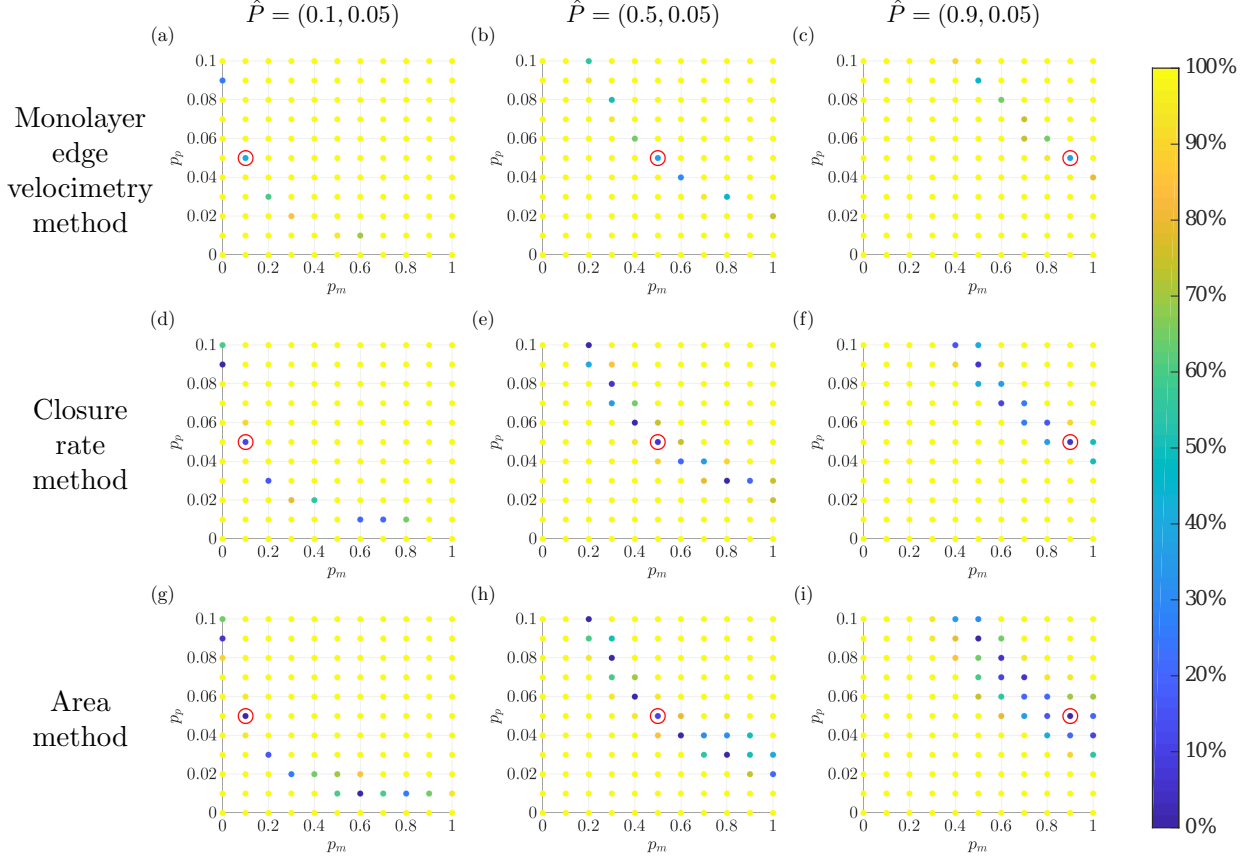

Figure S3: Series of plots showing how the performance of the three quantification methods changes as the motility rate of the focal parameters varies with fixed proliferation probability $\hat{p}_p = 0.01$. In each plot, the color of the circle at each parameter pair (p_m, p_p) indicates the percentage of times the migration measurements associated with the parameter pair are statistically significantly different from those associated with the focal parameters $\hat{P}$. The focal parameters $\hat{P}$ are indicated by a red circle. The results reveal that the monolayer edge velocimetry method yields a better statistical classification than the other methods. We note also the performance of all three methods declines as the motility rate of the focal parameters $\hat{P}$ increases.
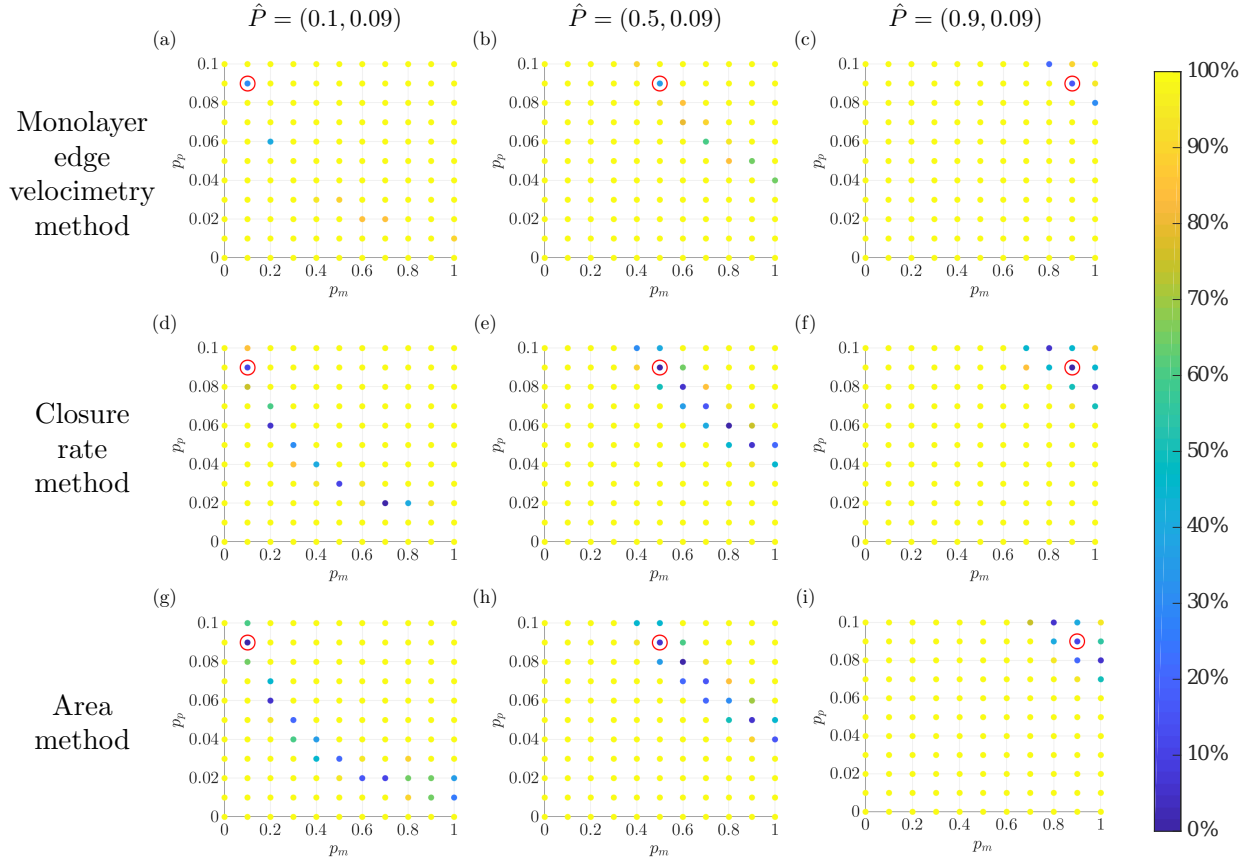
Figure S4: Series of plots showing how the performance of the three quantification methods changes as the motility rate of the focal parameters varies with fixed proliferation probability $\hat{p}_p = 0.09$. In each plot, the color of the circle at each parameter pair (p_m, p_p) indicates the percentage of times the migration measurements associated with the parameter pair are statistically significantly different from those associated with the focal parameters $\hat{P}$. The focal parameters $\hat{P}$ are indicated by a red circle. The results reveal that the monolayer edge velocimetry method yields a better statistical classification than the other methods. We note also the performance of all three methods declines as the motility rate of the focal parameters $\hat{P}$ increases.

S. 4 Determination of the optimal window size of the in vitro data

We present the plots of the objective function and the three fitness functions that contribute to its calculation, applied to the in vitro data.
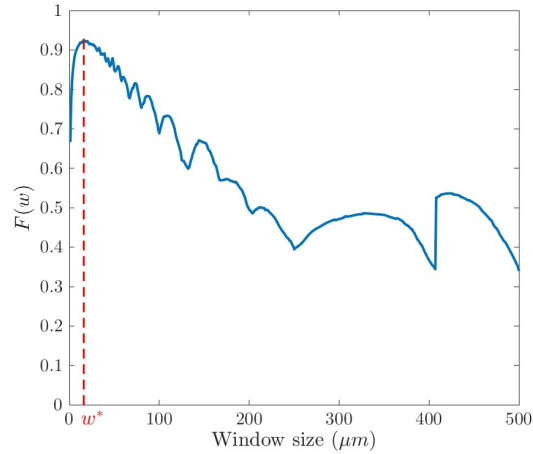

Figure S5: Plot of the objective function for the in silico data. The optimal window size, $w^* = 16$ μm is indicated with a dashed line in red.
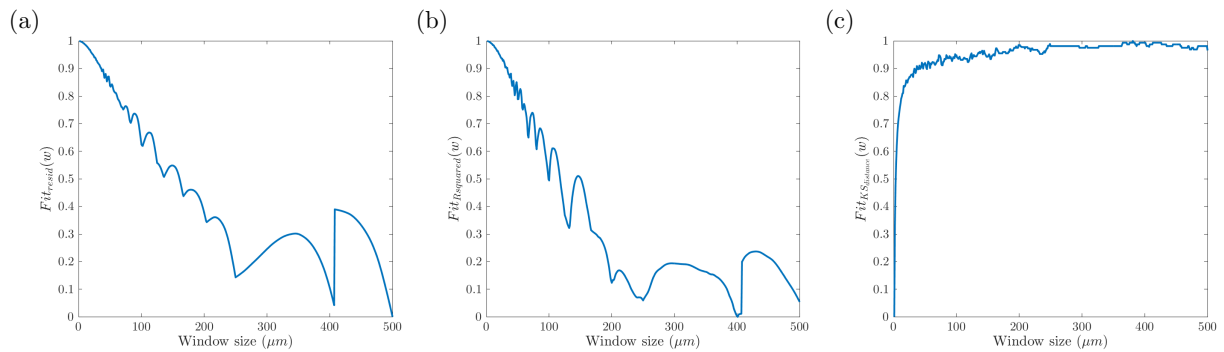

Figure S6: Plot of the fitness functions that constitute the objective function: (a) Fit_{resid}, (b) $Fit_{Rsquared}$ and (c) $Fit_{KS_{distance}}$. The functions have been rescaled so their values are between 0 and 1.

S. 5 Statistical classification of the in vitro data

We present the results of performing the unpaired two-sample t-test (t-test), the Wilcoxon rank-sum test and the two-sample Kolmogorov-Smirnov test (K-S test) between the migration measurements of the S1 group against the other groups' measurements. We fix a p-value < 0.05 to define statistical significance. We indicate in each row the statistical test performed and in each column we indicate if the hypothesis was rejected ($h = 1$) or not ($h = 0$), and the corresponding p-value for each hypothesis test.

	S2	S3	S4	S5	S6
t-test	h=1, p=1.101e-07	h=1, p=3.489e-46	h=1, p=5.102e-27	h=0, p=3.822e-01	h=0, p=1.026e-01
Wilcoxon rank sum test	h=1, p=3.626e-09	h=1, p=7.146e-41	h=1, p=4.907e-25	h=0, p=3.401e-01	h=0, p=4.520e-01
K-S test	h=1, p=4.026e-09	h=1, p=1.668e-33	h=1, p=5.865e-18	h=0, p=1.041e-01	h=1, p=1.093e-02

Table S2: Hypothesis test results comparing S1 and the other group's windowed velocities. In each row the statistical test performed is indicated.

	S2	S3	S4	S5	S6
t-test	h=0, p=1.199e-01	h=0, p=6.562e-02	h=0, p=1.291e-01	h=0, p=8.490e-01	h=0, p=7.062e-01
Wilcoxon rank sum test	h=0, p=3.429e-01	h=1, p=2.857e-02	h=0, p=2.000e-01	h=0, p=6.857e-01	h=0, p=3.429e-01
K-S test	h=0, p=1.075e-01	h=1, p=1.107e-02	h=0, p=1.075e-01	h=0, p=5.344e-01	h=0, p=1.075e-01

Table S3: Hypothesis test results comparing S1 and the other group's closure rates. In each row the statistical test performed is indicated.

The evolution of the percentage wound area of each scratch assay during the course of the experiment is shown in Figure S7.
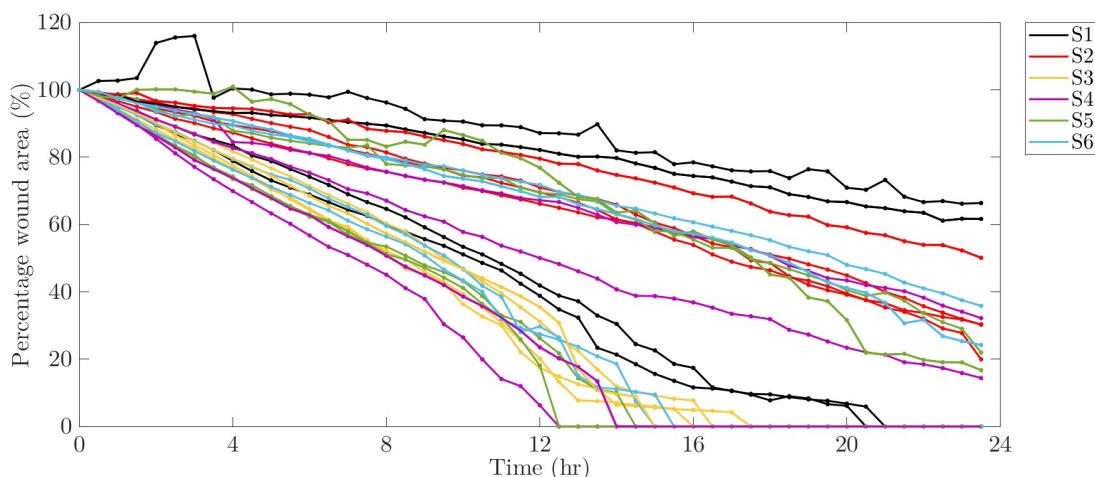

Figure S7: Evolution of the percentage wound area during the course of the experiment of each scratch assay. Experiments of the same cell group are plotted with the same color.

We calculated the time of comparison for the different groups, and the results are presented in Table S7.

	S2	S3	S4	S5	S6
Time of comparison (hr)	21	15	13	13	15

Table S4: Comparison times for the wound percentage areas of the different groups. The time of comparison was set to be half the time it takes for the first scratch being compared in which the leading edges touch.

The wound percentage area at the comparison times are shown in Figure S8.

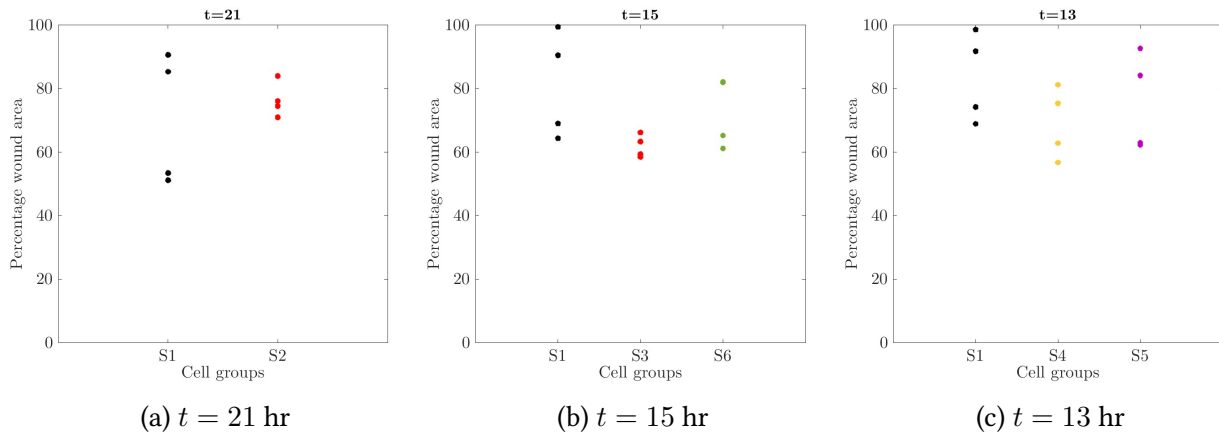| (a) $t = 21$ hr	(b) $t = 15$ hr	(c) $t = 13$ hr

Figure S8: Percentage wound area between S1 and the other groups at the time of comparison.

The results of the statistical tests applied to the percentage wound area at the time of comparison are shown in Table S5.

	S2	S3	S4	S5	S6
t-test	h=0, p=5.819e-01	h=0, p=6.936e-02	h=0, p=1.632e-01	h=0, p=4.790e-01	h=0, p=4.447e-01
Wilcoxon rank sum test	h=0, p=1.000e+00	h=0, p=5.714e-02	h=0, p=3.429e-01	h=0, p=4.857e-01	h=0, p=4.857e-01
K-S test	h=0, p=5.344e-01	h=0, p=1.075e-01	h=0, p=5.344e-01	h=0, p=5.344e-01	h=0, p=5.344e-01

Table S5: Hypothesis test results comparing S1 and the other group's percentage wound areas. In each row the statistical test performed is indicated.

References

[1] M. Bonamente. *Statistics and analysis of scientific data.* Springer, 2013.

[2] P. J. Brockwell, R. A. Davis, and M. V. Calder. *Introduction to time series and forecasting*, volume 2. Springer, 2002.

[3] P. J. Brockwell, R. A. Davis, and S. E. Fienberg. *Time Series: Theory and Methods: Theory and Methods.* Springer Science & Business Media, 1991.

[4] R. Fabbri and F. G. De León.   A statistical distance derived from the kolmogorov-smirnov test: specification, reference measures (benchmarks) and example uses.   *arXiv preprint arXiv:1711.00761*, 2017.